



# A spatiotemporal classification approach to evaluate the impacts of land use and land cover changes before and after the Três Irmãos reservoir formation in the Tietê River, Brazil

Beatriz Cirino Lucchetta<sup>1</sup> · Fernanda Sayuri Yoshino Watanabe<sup>1,2</sup> · Nariane Marselhe Ribeiro Bernardo do Carmo<sup>3</sup>

Received: 21 October 2022 / Accepted: 20 February 2023 / Published online: 13 March 2023  
© The Author(s), under exclusive licence to Springer Nature Switzerland AG 2023

## Abstract

Land use and land cover (LULC) maps are relevant tools to recognize deep changes in the natural landscape and direct strategies to minimize environmental impacts, being an important apparatus to obtain useful information in making decision by managers from watershed committees, political leaders and environmental agencies. Using Landsat multispectral images, this study aimed to investigate the changes in LULC of a watershed, influenced by the construction of the dam of the Três Irmãos hydroelectric plant, located in the low course of the Tietê River. The images were acquired in 1990, 2000, 2010 and 2018, which covers the periods before and after the flood caused by the dam build. For each date, LULC maps were generated using the supervised classification Maximum Likelihood (ML) algorithm. Those analysis has allowed identify possible influences of the reservoir formation over LULC in the watershed. A deep analysis showed a significant change of natural vegetation were flooded due to the damming, being partially recovered, in percentage terms, over time around the new watercourse. This study presents a reduction of 67% in the natural vegetation area from 1990 to 2000, while there was an increase of 35,36% between 2000 and 2018, when compared to the area occupied by natural vegetation existing in 1990. In addition, areas of natural vegetation also have been replaced by cultivated areas, which are predominant in the watershed.

**Keywords** Land use and land cover · Change detection · Image classification · Environmental monitoring · Watershed

## Introduction

Draining basins are territorial units, which correspond to extensions of a river and its tributaries, whose delimitation is a geological structure called watershed (Grannel-Pérez 2004). Large variations occur in land use and land cover (LULC) of watershed (Song et al. 2018), since several activities are developed around water resources, which impact geographic and physical environment and local societies (Salazar et al. 2015), such as urban expansion processes

(Shao et al. 2020), supply, energy generation and food production. The LULC dynamic is associated with the rearrangement activities and enterprises depending on the coverage type (FAO 2000). On the report of Brazilian Institute of Geography and Statistics (IBGE 2013), the LULC classification indicates a typology of use according to the geographic distribution, identified through homogeneous patterns of land cover.

Significant changes in surface cover derived from anthropogenic activities (Dibaba et al. 2020) can maximize negative effects on environmental resources, such as water quality and availability, being harmful to biodiversity and ecosystems (Guzha et al. 2018). Thus, the implementation of management policies and adaptation of priority uses of water (Tucci 1997) in conjunction with analyzes of LULC space–time dynamics are relevant for the management of water and land resources to achieve sustainable regional development (Feng et al. 2017). Activities whose have large-scale impact on the environment, in terms of surface coverage, are the constructions of dams for electricity generate (Lees et al. 2016), since river flows and geomorphology

✉ Fernanda Sayuri Yoshino Watanabe  
fernanda.watanabe@unesp.br

<sup>1</sup> Post-Graduation Program in Cartographic Sciences, Faculty of Sciences and Technology, São Paulo State University–UNESP, Presidente Prudente, SP 19060-900, Brazil

<sup>2</sup> Department of Cartography, Faculty of Sciences and Technology, São Paulo State University–UNESP, Presidente Prudente, SP 19060-900, Brazil

<sup>3</sup> Inspectral–Innovative Tecnology Solutions, Presidente Prudente, SP 19063-390, Brazil

of flooded areas are changed (Wu et al. 2018), including changes in landscape structure (Gage and Cooper et al. 2015), loss of ecosystems and biodiversity (Palmeirim et al. 2014) and expropriation of local people (Jafari and Hasheminasab 2017).

In Brazil, on the Tietê River lower course, the Três Irmãos dam was built to generate electricity, which has been in operation since 1993 (Eletrobrás Furnas 2022). Despite hydroelectric power generation being a renewable energy source, the construction dam caused environmental and social damage (Campos et al. 2018). The implementation of Três Irmãos reservoir in the Pereira Barreto caused population displacement and flooded part of the city, decharacterizing the local landscape. Besides many natural vegetation hectares and areas destined for agriculture were flooded, interfering with several ecosystems and the economy of the region (Campos et al. 2018). Recent works were not found which analyzed the LULC around the Três Irmãos watershed reservoir. However, acquiring information related to LULC, around flooded areas or reservoirs, due the dam build, are important to investigate the main influences of the built reservoir and to take decisions in environmental management policies (Yulianto 2016).

Remote sensing is an important approach to study the space–time dynamics of the LULC (Mamnun and Hossen 2020). The mapping and classification of LULC can be performed through photointerpretation of satellites images, whose objective is to identify and distinguish surface objects (Crósta 2002). Another widely used method is digital classification, where a target analysis is performed by objective interpretation, distinct from the subjectivity of a visual analysis. Furthermore, digital classification is able to collect data, seeking and extracting information quickly with satisfactory results (Venturieri and Santos 1998).

Recent works have been conducted to detect changes and map LULC using spatial and temporal resolution sensors such as satellites from Landsat (Hishe et al. 2021) and Sentinel (Silva 2020) constellations. The objective is to classify forests (Younis et al. 2022; Hossain et al. 2022), different soil types (Ma et al. 2023), urban areas (Ackom et al. 2020), agricultural surfaces (Sicre et al. 2020) and floodplains (Yulianto et al. 2016). In addition, different classification algorithms such as Maximun Likelihood (Araújo and Mamede 2021), Random Forest and Support Vector Machine (Ren et al. 2021) are tested. LULC studies aim to test whether sensors and classifications algorithms are suitable for detecting and classifying the earth's surface (Jia et al. 2014; Schulz 2021), as well as mapping space–time changes (Hussain et al. 2022; Hossain et al. 2023) to support policy decision-making in environmental management (Sarif and Gupta 2022), based on different classification systems (Gong et al. 2013).

The aim of this study was to investigate the evolution in LULC in the watershed of Três Irmãos hydroelectric plant, in order to find relationships between the LULC changes and the formation of reservoir. The Três Irmãos dam was the last to be built along the cascade of Tietê River reservoirs, in middle of 1990. Therefore, it was possible to find satellites images before and after the flood. A change detection assessment was applied in images based on the post-classification technique (Zhu 2017) to analyze the influence on LULC.

## Materials and methods

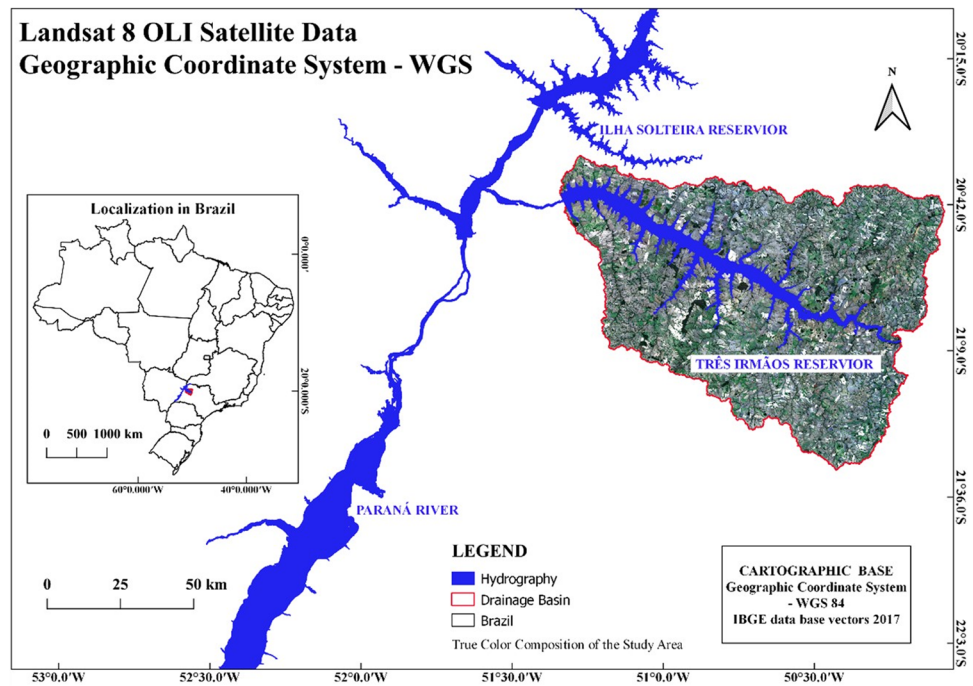
### Study area

The Três Irmãos reservoir watershed is located in Tietê River low course, in São Paulo State, Brazil (Fig. 1) and were developed for power generation. Worth mentioning the flooding reservoir processing has begun in August 1990, reaching its maximum volume in November 1990 (Eletrobrás Furnas 2022). The flooded area reaches 757 km<sup>2</sup> (Tijoá Energia 2020), average depth of 17.2 m (Barbosa et al. 1999) and useful volume of  $3.45 \times 10^3$  km<sup>3</sup> (CESP 2013). Três Irmãos reservoir is interconnect to the Ilha Solteira reservoir, located in the Paraná River, through Pereira Barreto channel, which is 9 km long and 61 m deep for navigation purpose between the Tietê and Paraná Rivers (Tijoá Energia 2020). According Campos et al. (2018), Três Irmãos reservoir brought economics benefits including an increase power generation capacity (807.5 MW) and energy security for the country, development to the region, population growth, expansion of urban industry, opening road, work, ecotourism and other activities related to the multiple uses of water. In accordance with the report by the Integrated Water Resources Management System of São Paulo State, the main activities developed in watershed are sugarcane crop and livestock and industries dependents on agriculture and animals' production.

### Acquisition and pre-processing of satellite images

Multispectral images were acquired from Landsat satellites between 1990 and 2018, comprising periods before and after the flooding of the Três Irmãos reservoir. The images are open source from United States Geological Survey (USGS) on the Earth Explorer webpage (<http://earthexplorer.usgs.gov/>) and were obtained from the sensors Thematic Mapper (TM–Landsat 5) and Operational Land Imager (OLI–Landsat 8), which have equivalent spatial and temporal resolutions for the visible bands of the electromagnetic spectrum. For both sensors, acquired products were Level-2, available in surface reflectance, whose atmospheric correction relied on Landsat 8 Surface Reflectance (L8SR) code, processed

**Fig. 1** Study area: Três Irmãos hydroelectric reservoir, located in the Tietê River, São Paulo State, Brazil



with Moderate Resolution Imaging Spectroradiometer–Climate Modeling Grid Aerosol (MODIS CMA) data (Vermote et al. 2016). The data were captured on 27 February 1990, 18 September 2000, 29 August 2010 and 18 July 2018.

To prevent the cloud effect in the image classification process, the satellite data were obtained in the seasonal period winter (July–September), except for the 1990 image that needed to match the period before the flood (February). In order to classify just the impact area, the images were crop using de boundaries of Três Irmãos reservoir watershed, delimited from digital elevation model (DEM), Suttle Radar Topography Mission (SRTM). The procedure of delimitation relies on the topography obtained from DEM/SRTM 1 Arc-Second Global data, also acquired on the Earth Explorer webpage.

### LULC classification and change detection

In this study, the maximum likelihood classification algorithm was used to generate discriminated functions for each LULC class (Table 1), based on statistical parameters to determine the probability of a pixel belonging to the class of interest (Richards 2013). For the maximum likelihood classifier, training samples were created considering the spectral signature to specify the land cover class, this classification technique was consolidated and widely applied to map LULC (Gong et al. 2013; Jia et al. 2014). The LULC classification and post-classification processes were performed in freely available QGIS software, version 2.18. By the maximum likelihood algorithm, the supervised classification was carried out using the Semi-Automatic

**Table 1** Land cover class name and description adapted of FAO (2000)

Class	Description
Artificial and natural water bodies (ANW)	Artificial water bodies areas covered by water due to the construction of artefacts such as reservoirs, canal, artificial lakes etc. Natural water bodies are areas naturally covered by water, such as lakes and rivers
Natural and semi-natural vegetation (NSNV)	Natural vegetated areas are defined as areas where the vegetative cover is in balance with the abiotic and biotic forces of its biotope. Semi-natural vegetation is defined as vegetation not planted by humans but influenced by human actions
Pasture (PA)	Areas of artificial vegetation planted to pasture
cultivated and managed terrestrial areas (CMTA)	Areas where the natural vegetation has removed or modified and replaced by other types of vegetative cover of anthropogenic origin. This vegetation is artificial and requires human activities
Bare soil areas (BSA)	Areas that do not have an artificial cover as a result of human activities. These areas include areas with less than 4% vegetative cover, bare rock areas, sands and desert

Classification Plugin (SCP) (Congedo et al. 2016) and the post-classification method (Zhu 2017) was performed using Land Cover Change tool, which makes comparative analyzes following classification pairs (time frames: 1990 and 2000; 2000 and 2010; 2010 and 2018; 1990 and 2018). Those analyzes quantify pixels changes for each class within the four time frames and they called pixel-by-pixel cross-tabulation (Jensen et al. 1987).

Five thematic classes were adopted according to the level-3 classes recommended by Land Cover Classification System (LCCS) of the Food and Agriculture Organization of United Nations (FAO), for land cover classification, listed hereafter as Artificial and Natural Bodies Water (ANW), Natural and Seminal Vegetation (NSNV), Pasture (PA), Cultivated and Managed Terrestrial Areas (CMTA) and Bare Soil Areas (BSA). To avoid an inconsistency classification, it was not considered a class for urban areas, since Landsat data have medium spatial resolution and cities in the impact area had small extensions.

How historical images were used, there is no possibility of carrying out field surveys to collect validation samples. Therefore, validation samples were explored from a high spatial resolution image projected in the Google Earth Pro tool, following the methodology mentioned by Olofsson et al. (2014). This methodology was applied only to the 2010 and 2018 data, since 1990 and 2000 Google Earth images presented spatial resolution equivalent to the images used in this work. The 1990 and 2000 classifications assessment were based on the original images. Thirty validation samples were selected from each class, which determined the “field truth”, to provide the confusion matrices and concordance coefficients.

### Classification accuracy

The classification was assessed using confusion matrices for each year investigated, two global metrics (i.e., overall accuracy and kappa coefficient) and two class-based metrics (i.e., user and producer accuracies). The overall accuracy was obtained from a set of test samples and was calculated by the ratio of correctly classified pixels and the total amount of pixels, being optimal when greater than 85% (Jensen 1986). On the other hand, kappa coefficient is a statistic measure of classification concordance, whose values range from zero (minimum concordance) to one (maximum concordance) (Congalton 1991). According to Foody (2020), kappa coefficient does not evaluate precision and its magnitude is difficult to interpret, since it is an index of agreement. Thus, to complement the approaches for calculating classification accuracy levels, user accuracy is related to commission errors, i.e., assigns pixels to classes to which they do not belong, while producer accuracy is related to omission

errors, i.e., represents the probability of a pixel being classified according to its attributes (Congalton 1991).

## Results and discussion

### LULC changes detection in the Tietê River watershed (1990 – 2018)

The LULC classifications for the years 1990, 2000, 2010 and 2018 of the study area are shown in the maps in Fig. 2, whose area statistics (in hectares and percentage) for respective years are summarized in Table 2. Comparing the maps in Fig. 2 through a first visual analysis, the CMTA land cover class remained predominant category for all the assessment periods. According to Trevisan et al. (2021), after the modernization of agricultural, livestock and industrial activities in 1970, it has been occurred an intense agricultural expansion in the Tietê river watershed, driven by the production of ethanol from sugarcane and others such as orange juice, vegetables oils, meat and milk.

In 1990, the ANW class accounted only 1% (5,172 ha) of the basin area, while the NSNV class covered 16% (139,463 ha). By that year, the others LULC categories followed the percentages: BSA 5% (42,308 ha), PA 21% (175,334) and CMTA 57% (488,670). This period corresponds to the moment before dam built and the flooded place for the generation of electric energy. By 2000, the flood caused due the dam construction expanded the ANW category for 58,758 ha, providing a 6% increase in the representativeness of the class in the study area. Meanwhile, the NSNV class showed a reduction of 93,456 ha, becoming the least representative category of the study area, with 5%. The flood covered an extensive region of Permanent Preservation Areas, with emphasis on riparian forests that were around the river. The PA class also suffered a significant reduction, about 12% compared to 1990. Despite CMTA class, in 2000, also has been partially flooded by the reservoir, a significant increase of 14% was observed, occupying 600,977 ha. The increase in water supply due to floods favors the water recirculation system from the rainy season to the dry season, providing advantages for large-scale agricultural production (Yoshida et al. 2020).

Although CMTA has exhibited a reduction in 2010, being the smallest area recorded for the class comparing the four dates, it remained the predominant watershed area. PA areas were increased, as a reflection of the reduction of CMTA areas. On the other hand, NSNV class showed an increase of 34,699 ha, since measures were implemented to recover riparian forests and policies to create legal reserves, such as Provisional Measure No. 2166–67, of 2001, in Brazil. In turn, BSA class kept practically unchanged, with an area of 66,879 ha. Based on analysis of 28-year Landsat data from the watershed impact area, the CMTA class remained

**Fig. 2** LULC classification maps for **a** 1990, **b** 2000, **c** 2010 and **d** 2018

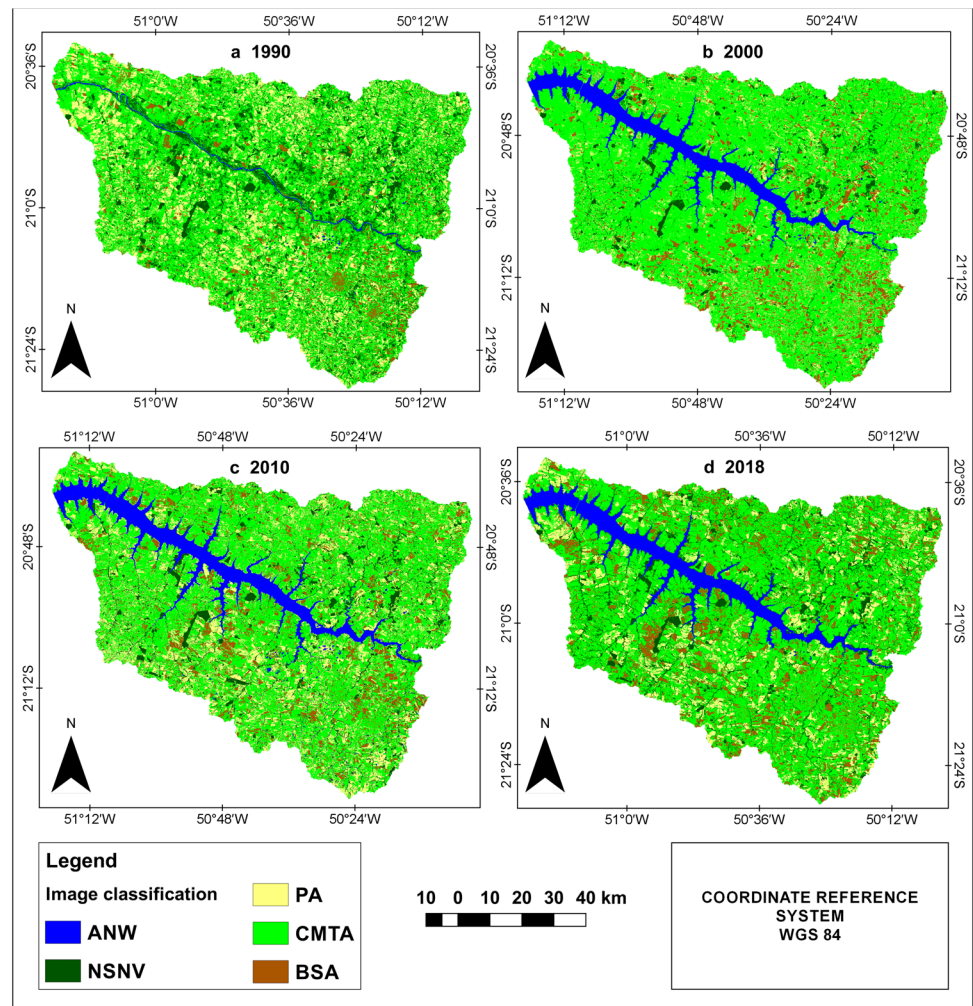


**Table 2** Area of each LULC (hectare e percentage) for 1990, 2000, 2010 and 2018

LULC	1990		2000		2010		2018	
	ha	%	ha	%	ha	%	ha	%
ANW	5,172	1	58,758	7	68,789	8	60,644	7
NSNV	139,463	16	46,007	5	80,706	9	95,305	11
PA	175,334	21	79,259	9	160,822	19	99,859	12
CMTA	488,670	57	600,977	71	473,751	56	507,367	60
BSA	42,308	5	65,945	8	66,876	8	87,771	10

dominant throughout the assessed period and its variation was inversely proportional to the PA class, since with the increase in the CMTA class, the PA class reduced. Ronquim and Fonseca (2018) suggesting the expansion of sugarcane cultivation areas has been replacing, preferably, pasture areas. Moreover, the NSNV showed an increase 49,298 ha since 2000, reaching 11% of the impact area.

The land cover change in percentage for each class is graphically presented in Fig. 3. The graphs have bars of different colors, the blue bars represent the unchanged areas, while the red bars represent areas that have been replaced

(lost) to other classes, in turn the green bars represent the areas that increased (gained). The change in land cover over the 28 years was dynamic and did not follow a set pattern. The NSNV and PA classes experienced negative changes, meanwhile CMTA remained a considerable percentage throughout the period. The fact of the flood have been occurred, due the hydroelectric plant built, conditions were crated to adapt the impact area for implantation of agricultura crops, since the reservoir have been supplid several activities.

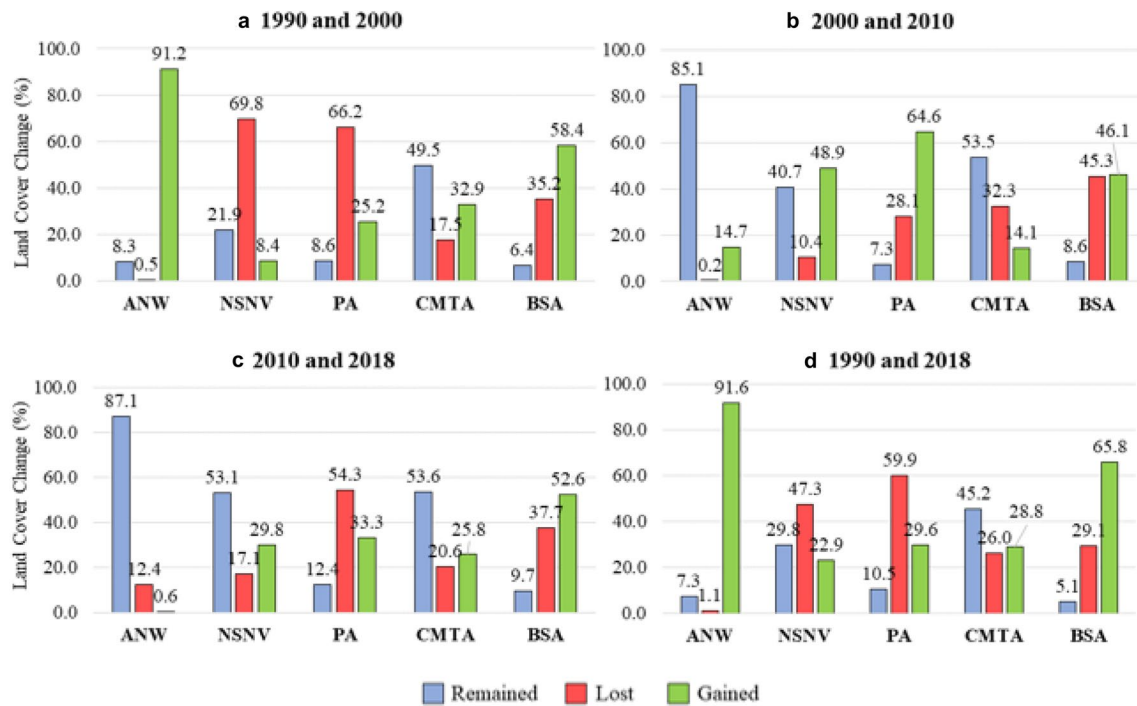


**Fig. 3** Graphical visualization of LULC change detection in percentage between the years **a** 1990 and 2000, **b** 2000 and 2010, **c** 2010 and 2018, **d** 1990 and 2018

Of these changes, the most impactful changes variations were observed in the first frame (1990–2000), being 91.2% gained of water, 69.8% lost of vegetation, 66.2% lost of pasture. Considering all period (1990–2018) BSA have been gained 65.8%. By the time, rates of NSNV were recovered into 2018, however, not reaching the amount of vegetation at the beginning of the time series. The period from 2010 and 2018 was tagged by the Brazilian Forest Code (Federal Law 4,771/1965, amended by Federal Law 12,651/2012) (Brazil 2012), which provides general rules for the protection of vegetation, including permanent preservation areas and legal reserves. Thereby, until 2018, the vegetation areas were environmentally compensated around the current watercourse, as determined by Forest Code.

Summarizing the changes in land cover from 28 years, classified images (1990–2018) were compared, resulting in a map (Fig. 4) to be observed the changes detection over the analyzed period. In the legend of the map, the class changes were clarified, presented by colors that show the categories changed from 1990 to 2018. From the changes, it was noted all classes were maintained in certain regions and other class changes did not occur (ANW to NSNV, ANW to PA, ANW to CMTA, ANW to BSA, BSA to ANW, BSA to NSNV). Those pairs of classes that did not show changes did not prevent the dynamicity of the impact area. Considering that part of the urban area of Pereira Barreto (class BSA) was flooded, no change detection was observed in the comparison map,

since the amount of changed area was not significant for the spatial resolution of the 30 m image.

The cross-tabulation of pixel-by-pixel approach, detailed in pixel percentage, assists in discerning LULC analyzes (Chowdhury et al. 2020). Cross-tabulation were applied for four different frames (1990–2000, 2000–2010, 2010–2018 and all period 1990–2018), presented in Tables 3, 4, 5, 6. During these periods the PA and BSA classes were mostly changed to the CMTA class, likewise the NSNV class in the first frame. Camara and Caldarelli (2016) explained that the expansion of sugarcane cultivation, due to the high demand for ethanol production, from 1990 onwards in the São Paulo State, mainly replaced other crops and pasture areas. Nevertheless, total recoverable sugar indicator (ATR) data, showed a growth rate of the product value was almost null from 1990/2000 and 2013/2014, with a big drop in sugar price in 2006/2007 and 2009/2010, which explains the replacement of agricultural crops by pasture, between 2000 and 2010, with 15.05%. Tables 4, 5, 6 presents that the NSNV class have been maintained a gradual increase in its areas (3.91, 4.31 and 7.17%, respectively), which was due to the application of vegetation maintenance policies.

**Fig. 4** LULC change detection over 28 years

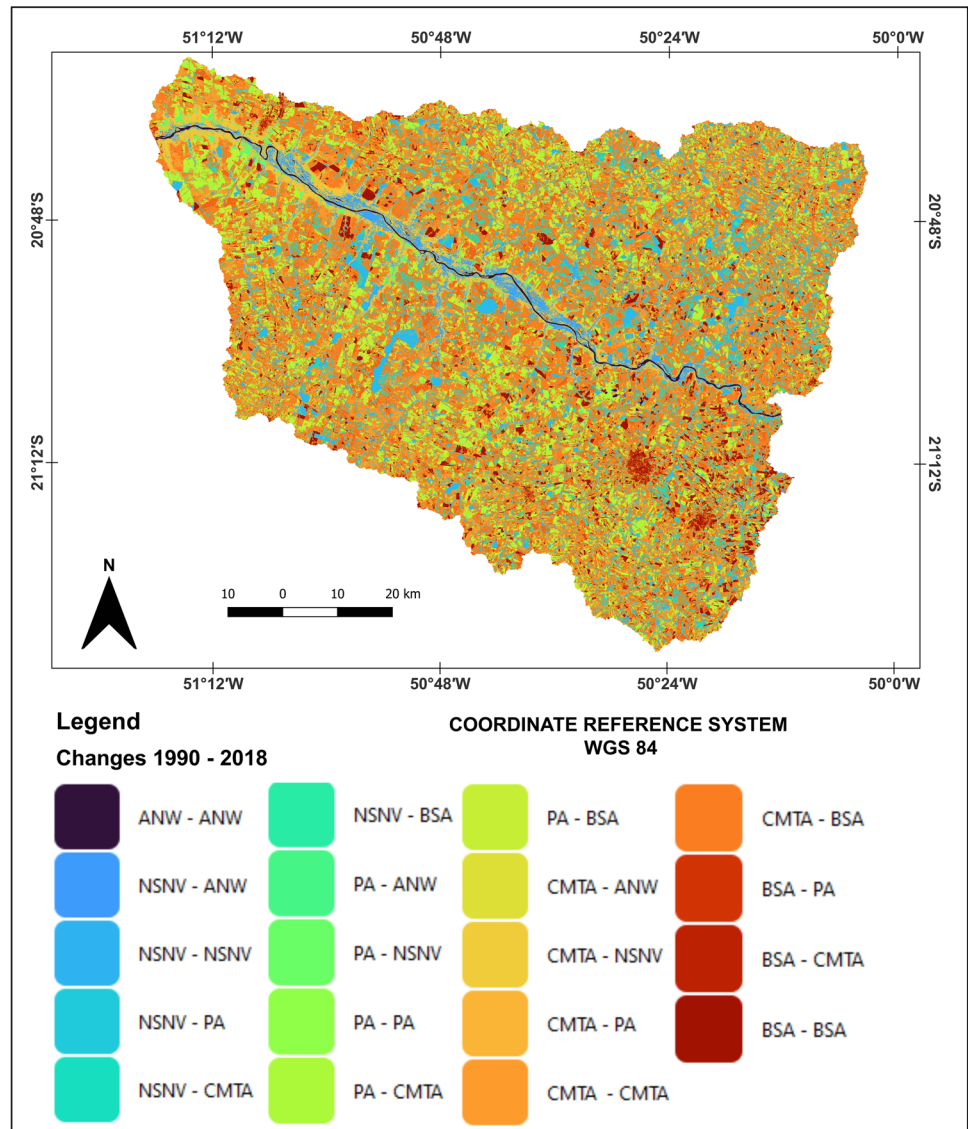


**Table 3** Cross-tabulation of LULC changes in pixel percentage (1990–2000)

Land Cover Change	ANW 1990	NSNV 1990	PA 1990	CMTA 1990	BSA 1990	Total
ANW 2000	0.57	2.22	0.50	3.48	0.14	6.91
NSNV 2000	0.00	3.91	0.07	1.28	0.14	5.41
PA 2000	0.00	0.67	2.38	5.64	0.63	9.31
CMTA 2000	0.03	9.04	15.86	42.41	3.29	70.62
BSA 2000	0.00	0.55	1.80	4.63	0.77	7.75
Total	0.61	16.39	20.60	57.43	4.97	100.00

**Image classification accuracy**

Evaluation accuracy is an important step to validate the maps resulting from the classification and corroborate the efficiency of the methodology applied in the study area (Congedo 2016). The confusion matrices are shown

in Tables 7, 8, 9, 10, as regard to the overall accuracy and the kappa coefficient are presented in Table 11, while the user accuracy and the producer accuracy are expressed in Table 12. The confusions regarding the classifications were not deep. In 1990, considering validation dataset, 2.64% of the CMTA pixels were classified as NSNV, 0.44% as PA, 0.41% as BSA and 0.65% of the NSNV pixels were classified

**Table 4** Cross-tabulation of LULC changes in pixel percentage (2000–2010)

Land cover change	ANW 2000	NSNV 2000	PA 2000	CMTA 2000	BSA 2000	Total
ANW 2010	6.89	0.06	0.02	1.10	0.01	8.08
NSNV 2010	0.00	4.31	0.19	4.89	0.10	9.48
PA 2010	0.00	0.34	1.91	15.05	1.60	18.90
CMTA 2010	0.01	0.63	6.20	44.04	4.81	55.67
BSA 2010	0.00	0.07	1.00	5.55	1.24	7.86
Total	6.91	5.41	9.31	70.62	7.75	100.00

**Table 5** Cross-tabulation of LULC changes in pixel percentage (2010–2018)

Land cover change	ANW 2010	NSNV 2010	PA 2010	CMTA 2010	BSA 2010	Total
ANW 2018	7.08	0.02	0.00	0.02	0.00	7.13
NSNV 2018	0.36	7.17	1.77	1.80	0.10	11.20
PA 2018	0.03	0.35	3.52	6.73	1.10	11.74
CMTA 2018	0.61	1.89	11.84	40.24	5.05	59.62
BSA 2018	0.01	0.05	1.76	6.88	1.61	10.31
Total	8.08	9.48	18.90	55.67	7.86	100.00

**Table 6** Cross-tabulation of LULC changes in pixel percentage (1990–2018)

Land Cover Change	ANW 1990	NSNV 1990	PA 1990	CMTA 1990	BSA 1990	Total
ANW 2018	0.53	2.30	0.53	3.63	0.15	7.13
NSNV 2018	0.01	6.33	0.41	4.26	0.18	11.20
PA 2018	0.00	1.08	3.08	7.07	0.50	11.74
CMTA 2018	0.06	6.08	13.65	36.43	3.40	59.62
BSA 2018	0.00	0.60	2.94	6.03	0.74	10.31
Total	0.61	16.39	20.60	57.43	4.97	100.00

**Table 7** Confusion matrix in pixel percentage of the year 1990

Class 1990	ANW	NSNV	PA	CMTA	BSA	Total
ANW	8.43	0.00	0.00	0.00	0.00	8.43
NSNV	0.00	51.78	0.00	2.64	0.00	54.42
PA	0.00	0.00	5.92	0.44	0.00	6.36
CMTA	0.00	0.65	0.00	20.62	0.00	21.26
BSA	0.00	0.00	0.00	0.41	9.11	9.52
Total	8.43	52.43	5.92	24.11	9.11	100.00

**Table 8** Confusion matrix in pixel percentage of the year 2000

Class 2000	ANW	NSNV	PA	CMTA	BSA	Total
ANW	80.81	0.00	0.00	0.00	0.00	80.81
NSNV	0.00	3.80	0.00	0.00	0.00	3.80
PA	0.00	0.00	1.56	0.05	0.00	1.61
CMTA	0.00	0.00	0.13	10.85	0.00	10.98
BSA	0.00	0.00	0.00	0.00	2.80	2.80
Total	80.81	3.80	1.69	10.90	2.80	100.00

as CMTA. Showed a satisfactory result, only 1.56% of the PA pixels were classified as CMTA and 0.13% of the CMTA pixels were classified as PA. As in previous reviews, the

year 2010 presented low pixels confusions, 1.52% of pixels that were CMTA areas were classified as PA areas, while 0.03% of the CMTA pixels were classified as NSNV areas.



**Table 9** Confusion matrix in pixel percentage of the year 2010

Class 2010	ANW	NSNV	PA	CMTA	BSA	Total
ANW	65.17	0.00	0.00	0.00	0.00	65.17
NSNV	0.00	11.98	0.00	0.03	0.00	12.01
PA	0.00	0.00	3.23	1.52	0.00	4.75
CMTA	0.01	0.00	0.00	7.05	0.00	7.06
BSA	0.00	0.00	0.00	0.00	11.01	11.01
Total	65.18	11.98	3.23	8.60	11.01	100.00

**Table 10** Confusion matrix in pixel percentage of the year 2018

Class 2018	ANW	NSNV	PA	CMTA	BSA	Total
ANW	34.10	0.00	0.00	0.00	0.00	34.10
NSNV	0.00	23.14	0.00	0.38	0.00	23.52
PA	0.00	0.00	3.72	2.41	0.00	6.14
CMTA	2.28	0.52	0.07	19.31	0.10	22.28
BSA	0.00	0.00	0.00	0.14	13.83	13.97
Total	36.38	23.66	3.79	22.24	13.93	100.00

**Table 11** Overall accuracy and kappa coefficient obtained for image classifications of different years

Image	Overall accuracy (%)	Kappa coefficient (0–1)
1990	95.86	0.935
2000	99.82	0.994
2010	98.44	0.971
2018	94.10	0.921

The image classification of 2018 exhibited the poorly results compared to the classifications from other years, 2.28% of the ANW pixels were classified as CMTA. Despite all the analyses, it is not possible to confirm the true surface target, since there were no field visits.

The methodology performed excellently, with overall accuracy greater than 94% and a kappa coefficient greater than 0.92, being the 2000 classification presenting the highest values, 99.82% and 0.994, respectively. About Table 12, despite most values of user accuracy were satisfactory, over 86%, PA class had an accuracy of 68.05% and 60.67% for 2010 and 2018, respectively. The confusion between PA and

CMTA classes was responsible for lowest user accuracy, since both classes may present similar spectral behaviors. Nonetheless, producer accuracy presented satisfactory values within the range 80–100%. The high accuracies found in this study are due to the adopted methodology. Several studies prove high accuracy with the use of the maximum likelihood for LULC classification (Araújo and Mamede 2021; Polat and Kaia 2021).

### Conclusion

This paper assessed the LULC changes in the watershed of the reservoir flooded by the Três Irmãos dam built, on the lower course of the Tietê River, for generate electricity, during 28 years (1990–2018), using multispectral images. From the findings, the area of interest was predominantly rural, where sugarcane production has been intensified for the ethanol generation. In the first decade of the assessment (1990–2010) 69.8% of vegetation areas were lost, as much of the vegetation in the impact area was flooded due to the construction of the reservoir. Despite this, from 2010 to 2018, the NSNV class was partially recovered

**Table 12** User accuracy and producer accuracy obtained after classification

Classes	User accuracy (%)				Producer accuracy (%)			
	1990	2000	2010	2018	1990	2000	2010	2018
ANW	100	100	100	100	100	100	99.99	93.74
NSNV	95.15	100	99.76	98.38	98.77	100	100	97.82
PA	93.09	97.03	68.05	60.67	100	92.34	100	98.18
CMTA	96.96	98.82	99.89	86.68	85.52	99.56	82.01	86.82
BSA	95.65	100	100	99.02	100	100	100	99.26

through the application of public policies and federal laws for the maintenance and conservation of vegetation. In addition to the areas of natural vegetation, a great dynamic was noted between agricultural areas and the pasture class, which showed gradual reductions and increases by years. Understanding the dynamic of the LULC over the years becomes an allowance for managers to elaborate and implement policies of environmental planning, land use planning, natural resource management and ecosystem services. We recommend improved monitoring for forested areas and policies for restoring natural vegetation. Furthermore, care is needed so that areas of natural vegetation are not replaced by agricultural areas, due to their importance.

**Acknowledgements** The authors thank FAPESP (grant N. 2017/24054-3) by Scientific Initiation scholarship and São Paulo State University.

**Data availability** The datasets gathered and generated in this study will be shared after reasonable request.

## Declarations

**Conflict of interest** On behalf of all authors, it is stated that there is no conflict of interest.

## References

- Ackom E, Adjei K, Odai S (2020) Monitoring land-use and land-cover changes due to extensive urbanization in the Odaw River Basin of Accra, Ghana, 1991–2030. *Mod Earth Syst Environ* 6:1131–1143. <https://doi.org/10.1007/s40808-020-00746-5>
- Araújo E, Mamede G (2021) Validation of soil uses around reservoirs in the semi-arid through image classification. *Revista Caatinga* 34(3):670–681. <https://doi.org/10.1590/1983-21252021v34n319rc>
- Barbosa F, Padisák J, Espíndola E, Borics G, Rocha O (1999) The cascading reservoir continuum concept (CRCC) and its application to the river Tietê-basin, São Paulo State, Brazil. *Theoret Reserve Ecol Appl* 22:425–437
- Instituto Brasileiro de Geografia e Estatística – IBGE (2013) Manual Técnico de Uso da Terra, pp. 17, Rio de Janeiro. <https://biblioteca.ibge.gov.br/visualizacao/livros/liv81615.pdf>. Accessed: May 21 2020.
- Brazil (2012) Federal Law nº 12.651. Forest Code. [http://www.planalto.gov.br/ccivil\\_03/leis/l4771.htm](http://www.planalto.gov.br/ccivil_03/leis/l4771.htm). Accessed 20 October 2022.
- Camara M, Caldarelli C (2016) Expansão canavieira e o uso da terra no estado de São Paulo. *Estudos Avançados* 30(88):93–116
- Campos L, Ferreira J, Oliveira B (2018) Impactos na construção de usinas hidrelétricas: um estudo de caso no complexo de Urubupungá. In: XIX Encontro Nacional de Geógrafos *João Pessoa, Paraíba*.
- Chowdhury M, Hasan M, Abdullah-Al-Mamun M (2020) Land use/land cover change assessment of Halda watershed using remote sensing and GIS. *Egypt J Remote Sens Space Sci* 23(1):63–75. <https://doi.org/10.1016/j.ejrs.2018.11.003>
- Congalton R (1991) A review of assessing the accuracy of classification remotely sensed data. *Remote Sens Environ* 37:35–36. [https://doi.org/10.1016/0034-4257\(91\)90048-B](https://doi.org/10.1016/0034-4257(91)90048-B)
- Congedo L (2016) Semi-automatic classification plugin documentation. Release 4(1):29. <https://doi.org/10.21105/joss.03172>
- Crósta A (2002) *Processamento Digital de Imagens de Sensoriamento Remoto*. Newyork, Campinas, p 170
- Companhia Energética de São Paulo – CESP (2013) Concessão da Usina Hidrelétrica Três Irmãos. [http://www2.aneel.gov.br/aplicacoes/consulta\\_publica/documentos/](http://www2.aneel.gov.br/aplicacoes/consulta_publica/documentos/). Accessed: 5 July 2019.
- Dibaba W, Demissie T, Miegel K (2020) Watershed hydrological response to combined land use/land cover and climate change in highland Ethiopia: Finchaa catchment. *Water* 12(6):1801. <https://doi.org/10.3390/w12061801>
- Eletrobras Furnas (2022) Usina Três Irmãos – 807,5 MW. <https://www.furnas.com.br/subsecao/135/usina-tres-irmaos---8075-mw?cultura=pt>. Accessed: 17 Jan 2022.
- Feng Y, Lu D, Moran E, Dutra L, Calvi M, De Oliveira M (2017) Examining spatial distribution and dynamic change of urban land covers in the Brazilian Amazon using multitemporal multisensor high spatial resolution satellite imagery. *Remote Sensing* 9(4):381. <https://doi.org/10.3390/rs9040381>
- Food and Agriculture Organization of the United Nations – FAO (2000) Land cover classification system (LCCS): classification concepts and user manual. <https://www.fao.org/3/x0596e/x0596e00.htm>. Accessed: 5 July 2019.
- Foody G (2020) Explaining the unsuitability of the kappa coefficient in the assessment and comparison of the accuracy of thematic maps obtained by image classification. *Remote Sens Environ* 239:0034–4257. <https://doi.org/10.1016/j.rse.2019.111630>
- Gage E, Cooper D (2015) The influence of land cover, vertical structure, and socioeconomic factors on outdoor water use in a western US City. *Water Resour Manage* 29:3877–3890. <https://doi.org/10.1007/s11269-015-1034-7>
- Gong P, Wang J, Yu L, Zhao Y, Zhao Y, Liang L, Niu Z, Huang X, Fu H, Liu S, Li C, Li X, Fu W, Liu C, Xu Y, Wang X, Cheng Q, Hu L, Yao W, Zhang H, Zhu P, Zhao Z, Zhang Z, Zheng Y, Ji L, Zhang Y, Chen H, Yan A, Guo J, Yu L, Wang L, Liu X, Shi T, Zhu M, Chen Y, Yang G, Tang P, Xu B, Giri C, Clinton N, Zhu Z, Chen J, Chen J (2013) Finer resolution observation and monitoring of global land cover: first mapping results with Landsat TM and ETM+ data. *Int J Remote Sens* 34(7):2607–2654. <https://doi.org/10.1080/01431161.2012.748992>
- Grannel-Pérez M (2004) *Trabalhando geografia com cartas topográficas*. Unijuí, Ijuí
- Guzha A, Rufino M, Okoth S, Jacobs S, Nóbrega R (2018) Impacts of land use and land cover change on surface runoff, discharge and low flows: Evidence from East Africa. *J Hydrol Reg Stud* 15:49–67. <https://doi.org/10.1016/j.ejrh.2017.11.005>
- Hishe H, Giday K, Orshoven J, Muys B, Taheri F, Azadi H, Feng L, Zamani O, Mirzaei M, Witlox F (2021) Analysis of land use land cover dynamics and driving factors in desa’a forest in northern ethiopia. *Land Use Policy* 101:0264–8377. <https://doi.org/10.1016/j.landusepol.2020.105039>
- Hossain A, Masiero M, Pirotti F (2022) Land cover change across 45 years in the world’s largest mangrove forest (Sundarbans): the contribution of remote sensing in forest monitoring. *Euro J Remo Sens*. <https://doi.org/10.1080/22797254.2022.2097450>
- Hossain M, Khan M, Oluwajuwon T, Biswas J, Abdullah RS, Tanvir M, Munira S, Chowdhury M (2023) Spatiotemporal change detection of land use land cover (LULC) in Fashiakhali wildlife sanctuary (FKWS) impact area, Bangladesh, employing multispectral images and GIS. *Model Earth Syst Environ*. <https://doi.org/10.1007/s40808-022-01653-7>
- Hussain S, Lu L, Mubeen M, Nasim W, Karuppannan S, Fahad S, Tariq A, Mousa BG, Mumtaz F, Aslam M (2022) Spatiotemporal variation in land use land cover in the response to local climate change using multispectral remote sensing data. *Land* 11(5):595. <https://doi.org/10.3390/land11050595>
- Jafari R, Hasheminasab S (2017) Assessing the effects of dam building on land degradation in central Iran with Landsat LST and LULC time series. *Environ Monit Assess* 189:1–15. <https://doi.org/10.1007/s10661-017-5792-y>

- Jensen J (1986) *Introductory digital image processing*. Prentice Hall, Englewood Cliffs
- Jensen J, Ramsey E, Mackey H, Christensen E, Sharitz R (1987) Inland wetland change detection using aircraft MSS data. *Photogramm Eng Remote Sens* 53(5):521–529
- Jia K, Wei X, Gu X, Yao Y, Xie X, Li B (2014) Land cover classification using Landsat 8 Operational Land Imager data in Beijing. *China Geocarto Int* 29(8):941–951. <https://doi.org/10.1080/10106049.2014.894586>
- Lees A, Peres C, Fearnside P, Schneider M, Zuanon J (2016) Hydro-power and the future of Amazonian biodiversity. *Biodivers Conserv* 25:451–466. <https://doi.org/10.1007/s10531-016-1072-3>
- Ma S, Wang L, Wang H, Zhao Y, Jiang J (2023) Impacts of land use/land cover and soil property changes on soil erosion in the black soil region. *China. J Environ Manag.* 328:117024
- Mamnun M, Hossen S (2020) Spatio-temporal analysis of land cover changes in the evergreen and semi-evergreen rainforests: a case study in Chittagong Hill Tracts. Bangladesh. *Int J for Ecol Environ.* 2:87–99
- Olofsson P, Foody G, Herold M, Stehman S, Woodcock C, Wulder M (2014) Good practices for estimating area and assessing accuracy of land change. *Remote Sens Environ* 148(3):42–57. <https://doi.org/10.1016/j.rse.2014.02.015>
- Palmeirim A, Peres C, Rosas F (2014) Giant otter population responses to habitat expansion and degradation induced by a mega hydroelectric dam. *Biol Cons* 174:30–38. <https://doi.org/10.1016/j.biocon.2014.03.015>
- Polat N, Kaya Y (2021) Investigation of the Performance of Different Pixel-Based Classification Methods in Land Use/Land Cover (LULC) Determination. *Türkiye İnsansız Hava Araçları Dergisi.* 3(1):1–6
- Ren J, Shao Y, Wan H, Xie Y (2021) Campos A (2021) A two-step mapping of irrigated corn with multi-temporal MODIS and Landsat analysis ready data. *ISPRS J Photo Remote Sens* 176:69–82. <https://doi.org/10.1016/j.isprsjprs.2021.04.007>
- Richards J (2013) *Remote Sensing Digital Image Analysis*. Springer, Canberra
- Ronquim C, Fonseca M (2018) Avanço das áreas de cana-de-açúcar e alterações em áreas de agropecuária no interior paulista. *Campinas.* 48:0103–7811
- Salazar S (2015) Lógicas territoriales y relaciones de poder en el espacio de dos actores armados: un aporte de la geografía política al estudio de la violencia y el conflicto armado en Colombia. *Cuadernos De Geografía.* 24(1):157–172
- Sarif M (2022) Gupta R (2022) Spatio-temporal mapping of land use/land cover dynamics using Remote Sensing and GIS approach: a case study from the city of Prayagraj, India (1988–2018). *Environ Dev Sustain* 24:888–920. <https://doi.org/10.1007/s10668-021-01475-0>
- Schulz D, Yin H, Tischbein B, Verleysdonk S, Adamou R, Kumar N (2021) Land use mapping using Sentinel-1 and Sentinel-2 time series in a heterogeneous landscape in Niger. *Sahel ISPRS J Photogramm Remote Sens* 178:97–111. <https://doi.org/10.1016/j.isprsjprs.2021.06.005>
- Shao Z, Bakker M, Spit T, Janssen-Jansen L, Qun W (2020) Containing urban expansion in China: the case of Nanjing. *J Environ Plan Man* 63(2):189–209. <https://doi.org/10.1080/09640568.2019.1576511>
- Sicre C, Fieuzal R, Baup F (2020) Contribution of multispectral (optical and radar) satellite images to the classification of agricultural surfaces. *Inter J Appl Earth Obser Geoinform* 84:101972. <https://doi.org/10.1016/j.jag.2019.101972>
- Silva I (2020) Avaliação de metodologias de aprendizagem automática na classificação de culturas agrícolas com base em imagens do Sentinel-2. Universidade de Lisboa, Dissertation
- Song X, Hansen M, Stehman S, Peter V, Alexandra T, Eric F, John R (2018) Global land change from 1982 to 2016. *Nature* 560:639–643. <https://doi.org/10.1038/s41586-018-0411-9>
- Tijoa Energia (2020) Usina Hidrelétrica Três Irmãos, Andradina/SP. <http://www.tijoa.com>. Accessed: 11 May 2021.
- Trevisan D, Bispo P, Gou Y, Souza B, Liesenberg V, Harris A, Balzter H, Moschini L (2021) Analysis of a landscape intensely modified by agriculture in the tietê-jacaré watershed. *Brazil Sustainability* 13(16):9304. <https://doi.org/10.3390/su13169304>
- Tucci C (1997) *Hidrologia: ciência e aplicação*. Editora da Universidade, Porto Alegre
- United States Geological Survey – USGS (2018) Earth Explorer. <https://earthexplorer.usgs.gov/>. Accessed 10 Sept 2018
- Venturieri A, Santos J (1998) Técnicas de classificação de imagens para análise de cobertura vegetal. In: Assad E, Sano E (eds) *Sistema de informações geográficas: aplicações na agricultura*. Brasília
- Vermote E, Justice C, Claverie M, Franch B (2016) Preliminary analysis of the performance of the Landsat 8/OLI land surface reflectance product. *Remote Sens Environ* 185:46–56. <https://doi.org/10.1016/j.rse.2016.04.008>
- Wu Z, Milliman J, Zhao D, Cao Z, Zhou J, Zhou C (2018) Geomorphologic changes in the lower Pearl River Delta, 1850–2015, largely due to human activity. *Geomorphology* 314:42–54. <https://doi.org/10.1016/j.geomorph.2018.05.001>
- Yoshida Y, Lee H, Trung B, Tran H, Lall M, Kakar K, Xuan T (2020) Impacts of mainstream hydropower dams on fisheries and agriculture in lower Mekong Basin. *Sustainability* 12(6):2408. <https://doi.org/10.3390/su12062408>
- Younis A, Jonathan B, Togun A, Yasin E, Omer S, Hamad G, Aissata S (2022) Assessment of land use and land cover change on Gum Talha forest in Bahar Alarab Sudan. *Biod J Biol Diver.* 23:922
- Yulianto F, Prasasti I, Pasaribu J, Fitriana H, Haryani N, Sofan P (2016) The dynamics of land use/land cover change modeling and their implication for the flood damage assessment in the Tondano watershed, North Sulawesi, Indonesia. *Mod Earth Syst Environ* 2:1–20. <https://doi.org/10.1007/s40808-016-0100-3>
- Zhu Z (2017) Change detection using Landsat time series: A review of frequencies, preprocessing, algorithms, and applications. *ISPRS J Phot Remo Sens* 130:370–394. <https://doi.org/10.1016/j.isprsjprs.2017.06.013>

**Publisher's Note** Springer Nature remains neutral with regard to jurisdictional claims in published maps and institutional affiliations.

Springer Nature or its licensor (e.g. a society or other partner) holds exclusive rights to this article under a publishing agreement with the author(s) or other rightsholder(s); author self-archiving of the accepted manuscript version of this article is solely governed by the terms of such publishing agreement and applicable law.